THE PUBLISHING HOUSE
OF THE ROMANIAN ACADEMY

PROCEEDINGS OF THE ROMANIAN ACADEMY, Series A,
Volume 23, Number 3/2022, pp. 269–277

UNSTEADY MHD NANOFLUID CONVECTION WITH HEAT TRANSFER OVER A STRETCHING AND VERTICALLY MOVING SHEET

Khodani Sherrif TSHIVHI, Oluwole Daniel MAKINDE, Ramotjaki Lucky MONALEDI

Stellenbosch University, Faculty of Military Science, Private Bag X2, Saldanha 7395, South Africa
Corresponding author: Khodani Sherrif TSHIVHI, E-mail: khodani.tshivhi@gmail.com

Abstract. This study examines the combined effects of magnetic field, viscous dissipation and Joule heating on inherent irreversibility in an unsteady stagnation point flow of a conducting Cu-water nanofluid towards a convectively heated stretching and vertically moving slippery sheet. Based on some realistic assumptions, the nonlinear differential equations governing the single phase nanofluid flow model problem is obtained and numerically tackled via shooting technique coupled with the Runge-Kutta-Fehlberg integration scheme. Pertinent results depicting the effects of various emerging parameters on the nanofluid velocity and temperature profiles together with the skin friction, Nusselt number, entropy generation rate and Bejan number are graphically displayed and quantitatively discussed. It was found that the total entropy generation rate escalates with a rise in the nanofluid volume fraction, sheet surface convective heating, magnetic field and sheet vertical motion while an upsurge in the surface slipperiness lessens it.

Keywords: magnetohydrodynamics (MHD), stretching and vertically moving sheet, unsteady nanofluid flow, viscous dissipation, Joule heating, entropy generation rate.

1. INTRODUCTION

Recent advancement in nanotechnology coupled with the challenging problem of thermal management in industrial and engineering systems warrant the need for an ultra-heat transfer fluid with significantly higher thermal conductivity. The concept and development of nanofluids pioneered by Choi [1] are directly related to uptrends in the miniaturization of nanotechnology due to its improved thermal conductivity. To investigate the heat transfer enhancement capability of nanofluids, precise values of physical and thermal properties are required such as specific heat capacity, viscosity, density, electrical conductivity, and thermal conductivity [2–4]. Theoretical and experimental studies on nanofluids convection with heat transfer enhancement characteristics have received attention from several authors [5–8]. Moreover, the interaction between electrical conducting nanofluid and the magnetic field known as magnetohydrodynamic (MHD) has also received great consideration among researchers due to its importance and many practical applications in manufacturing and chemical processes industries [9–14]. Annar *et al*. [15] conducted a study on MHD flow past a nonlinear stretching/shrinking sheet in carbon nanotubes. They reported the existence of dual solutions in the case of shrinking sheet and perform a stability analysis in order to determine the realistic solution to the problem. Later, Tadesse *et al*. [16, 17] studied the problem of hydromagnetic stagnation point flow of a magnetite ferrofluid past a convective heated permeable stretching/shrinking sheet in a Darcy-Forchheimer porous medium with or without buoyancy forces. Their results also revealed the existence of dual solutions in the shrinking sheet regime. Nandi *et al*. [18] theoretically examined the MHD stagnation point flow of Fe_3O_4/Cu/Ag-CH_3OH nanofluid along with a convectively heated stretching sheet with partial slip and activation energy. Their results revealed the heat transfer enhancement capacity of different nanoparticles involved. The impact of magnetic dipole on the performance-based of Yamada Ota and Hamilton Crosser hybrid nanofluid convection past a stretched surface was examined by Gul *et al*. [19]. Khashi'ie *et al.* [20] investigated the influence of magnetic field on thermal boundary layer of an electrically conducting hybrid nanofluid over a moving plate.

In the present study, the recent work of Tshivhi and Makinde [21] is extended to include entropy generation analysis in an unsteady MHD nanofluid convection with heat transfer over a stretching and vertically moving sheet. According to the authors' information and reviews, no research has been done on this problem geometry before and the current work is considered to fill the gap in the literature. In the following sections, relevant governing equations are obtained and transformed into ordinary differential equations using appropriate similarity variables. Shooting numerical procedure coupled with the Runge-Kutta-Fehlberg integration scheme are employed to tackle the model problem. Pertinent results depicting the effects of various emerging parameters on the velocity, temperature, skin friction, Nusselt number, entropy generation rate and Bejan number are graphically displayed and discussed. The results revealed that the upward/downward motion of a stretching sheet can be significant with regard to the flow structure, heat transfer and entropy generation features.

2. MODEL PROBLEM

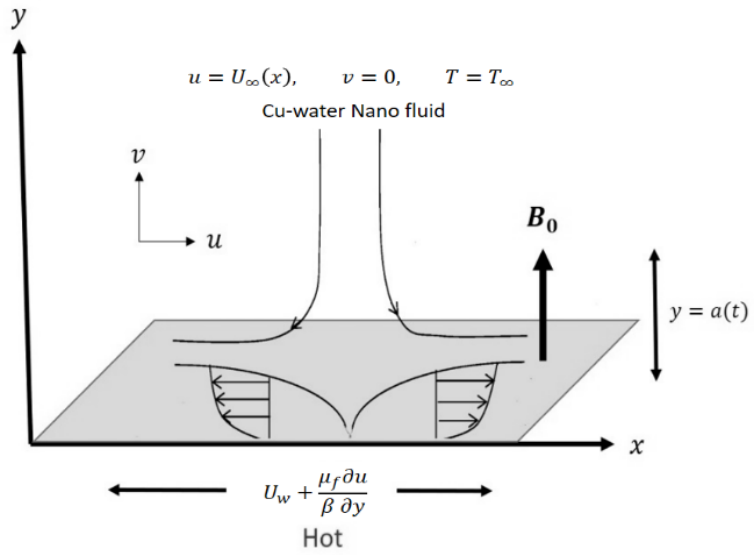

Fig. 1 – Schematic view of the model.

Consider a two-dimensional unsteady stagnation point flow of a viscous incompressible and electrically conducting water base nanofluid containing Copper (Cu) nanoparticles, towards a convectively heated and vertically moving stretching sheet with a slippery surface, as shown in Figure 1. A uniform magnetic field with strength B_0 is imposed in the positive y-direction. Using the boundary layer approximation, the governing equations of continuity, momentum, energy and entropy generation rate may be written in the usual notation as [10–21]

$$\frac{\partial u}{\partial x}+\frac{\partial v}{\partial y}=0, \tag{1}$$

$$\frac{\partial u}{\partial t}+u\frac{\partial u}{\partial x}+v\frac{\partial u}{\partial y}=U_\infty\frac{\mathrm{d}U_\infty}{\mathrm{d}x}+\frac{\mathrm{d}U_\infty}{\mathrm{d}t}+\frac{\mu_{nf}}{\rho_{nf}}\left(\frac{\partial^2 u}{\partial y^2}\right)\frac{\sigma_{nf}}{\rho_{nf}}B_0^2\left(u-U_\infty\right), \tag{2}$$

$$\frac{\partial T}{\partial t}+u\frac{\partial T}{\partial x}+v\frac{\partial T}{\partial y}=\frac{k_{nf}}{(\rho C_p)_{nf}}\frac{\partial^2 T}{\partial y^2}+\frac{\mu_{nf}}{(\rho C_p)_{nf}}\left(\frac{\partial u}{\partial y}\right)^2+\frac{\sigma_{nf}}{(\rho C_p)_{nf}}B_0^2\left(u-U_\infty\right)^2, \tag{3}$$

$$E_g=\frac{k_{nf}}{\left(T_f-T_\infty\right)^2}\left(\frac{\partial T}{\partial y}\right)^2+\frac{\mu_{nf}}{T_f-T_\infty}\left(\frac{\partial u}{\partial y}\right)^2+\frac{\sigma_{nf}}{T_f-T_\infty}B_0^2\left(u-U_\infty\right)^2, \tag{4}$$

subject to the boundary conditions,

$$y = a(t), \quad u = U_w + \frac{\mu_f}{\beta}\frac{\partial u}{\partial y}, \quad v = 0, \quad -k_f \frac{\partial T}{\partial y} = h_f\left(T_f - T(x,0)\right),$$
$$y \to \infty, \quad u = U_\infty, \quad v = 0, \quad T(x,\infty) \to T_\infty, \tag{5}$$

where (u,v) represent the velocity components along (x,y) directions in the Cartesian coordinates, t is the time, U_∞ is the free stream velocity, μ_{nf} is the nanofluid dynamic viscosity, ρ_{nf} is the nanofluid density, σ_{nf} is the nanofluid electrical conductivity, T is the temperature, k_{nf} is nanofluid thermal conductivity, $(\rho C_p)_{nf}$ is the specific heat capacity of nanofluid, E_g is the entropy generation rate, T_f is the temperate of the hot fluid beneath the sheet surface, T_∞ is the free stream temperature, U_w is the velocity of stretching surface, β is the slip length coefficient, k_f is the base fluid thermal conductivity, μ_f is the base fluid dynamic viscosity and h_f is the heat coefficient. The following similarity variables and parameters are introduced into equations (1)–(5):

$$\psi = x\sqrt{\frac{b\upsilon_f}{1+ct}}F(\xi), \quad \xi = y\sqrt{\frac{b}{\upsilon_f(1+ct)}} - 1, \quad u = \frac{xb}{1+ct}F'(\xi), \quad v = -\sqrt{\frac{b\upsilon_f}{1+ct}}F(\xi),$$
$$\theta = \frac{T - T_\infty}{T_f - T_\infty}, \quad U_\infty = \frac{bx}{1+ct}, \quad U_w = \frac{ax}{1+ct}, \quad a(t) = \sqrt{\frac{\upsilon_f(1+ct)}{b}}, \quad A_0 = \frac{\upsilon_f}{\upsilon_{nf}}, \quad A_1 = \frac{\sigma_{nf}\rho_f}{\sigma_f\rho_{nf}},$$
$$A_2 = \frac{k_f(\rho C_p)_{nf}}{k_{nf}(\rho C_p)_f}, \quad A_3 = \frac{\mu_{nf}k_f}{\mu_f k_{nf}}, \quad A_4 = \frac{\sigma_{nf}k_f}{\sigma_f k_{nf}}, \quad A_5 = \frac{k_{nf}}{k_f}, \quad A_6 = \frac{\mu_{nf}}{\mu_f}, \quad A_7 = \frac{\sigma_{nf}}{\sigma_f}, \quad S = \frac{c}{b}, \tag{6}$$
$$M = \frac{\sigma_f B_0^2}{\rho_f b}(1+\mathrm{ct}), \quad \mathrm{Pr} = \frac{\upsilon_f k_f}{(\rho C_p)_f}, \quad \mathrm{Ec} = \frac{U_\infty^2}{(C_p)_f\left(T_f - T_\infty\right)}, \quad N_s = \frac{E_g\upsilon_f(1+ct)}{bk_f}, \quad \lambda = \frac{a}{b},$$
$$L = \frac{\mu_f}{\beta}\sqrt{\frac{b}{\upsilon_f(1+ct)}}, \quad \mathrm{Bi} = -\frac{h_f}{k_f}\sqrt{\frac{\upsilon_f(1+ct)}{b}},$$

and we obtain

$$F'''(\xi) + A_0\left(F(\xi)F''(\xi) - F'(\xi)^2\right) + A_0 S\left(F'(\xi) + \frac{\xi+1}{2}F''(\xi)\right) - A_0A_1M\left(F'(\xi) - 1\right) + A_0\left(1 - S\right) = 0, \tag{7}$$

$$\theta''(\xi) + A_2(\mathrm{Pr})\left(F(\xi) + \frac{\xi+1}{2}\right)\theta'(\xi) + A_3(\mathrm{Pr})(\mathrm{Ec})F''(\xi)^2 + A_4(\mathrm{Pr})(\mathrm{Ec})M\left(F'(\xi) - 1\right)^2 = 0, \tag{8}$$

$$N_s = A_5\theta'(\xi)^2 + A_6(\mathrm{Pr})(\mathrm{Ec})F''(\xi)^2 + A_7(\mathrm{Pr})(\mathrm{Ec})M\left(F'(\xi) - 1\right)^2 = 0, \tag{9}$$

with the boundary conditions given as,

$$F(0) = 0, \quad F'(0) = \lambda + LF''(0), \quad \theta'(0) = -\mathrm{Bi}\left(1 - \theta(0)\right),$$
$$\theta(\infty) = 0, \quad F'(\infty) = 1, \tag{10}$$

where the constant A_0, A_1, A_2, A_3, A_4, A_5, A_6, and A_7 are defined in equation (6). The physical parameters of interest influencing the flow system are as follows: S represents the vertical movement of the surface, M is magnetic field parameter, Pr is the base fluid Prandtl number (Pr = 6.2), Ec is the Eckert number, N_s is the entropy generation rate, λ is the stretching parameter, L is the surface slip parameter, and Bi is the thermal Biot number. Other quantities of engineering interest are the skin friction coefficients C_f, the Nusselt number

Nu and the Bejan number Be, given as:

$$C_f\sqrt{\mathrm{Re}_x}=\frac{F''(0)}{(1-\phi)^{2.5}},\quad \frac{\mathrm{Nu}}{\sqrt{Re_x}}=-\frac{k_{nf}}{k_f}\theta'(0),\quad \mathrm{Be}=\frac{1}{1+\dfrac{N_2}{N_1}},$$
$$C_f=\frac{\tau_w}{\rho_f U_\infty^2},\quad Nu=\frac{xq_w}{k_f(T_f-T_\infty)},\quad T_w=\mu_{nf}\frac{\partial u}{\partial y}\Big|y=0,\quad \mathrm{Re}_x=\frac{xU_\infty}{\upsilon_f},\tag{11}$$
$$N_1=A_5\theta'(\xi)^2,\quad N_2=A_6(Pr)(Ec)F''(\xi)^2+A_7(\mathrm{Pr})(\mathrm{Ec})M\left(F'(\xi)-1\right)^2,$$

where the parameters τ_w is the sheet surface shear stress, q_w is the dimensional heat flux at sheet surface, Re_x is the local Reynolds number, ϕ is the nanofluid volume fraction, N_1 represents heat transfer irreversibility while N_2 is the irreversibility due to fluid friction and magnetic field.

Table 1

The relationship between nanoparticle and basefluids [10, 16, 18, 21]

Properties	Nanofluid
Density	$\rho_{nf}=(1-\phi)\rho_f+\phi\rho_s$
Heat Capacity	$(\rho C_p)_{nf}=(1-\phi)(\rho C_p)_f+\phi(\rho C_p)_s$
Viscosity	$\mu_{nf}=\dfrac{\mu_f}{(1-\phi)^{2.5}}$
Thermal Conductivity	$\dfrac{k_{nf}}{k_f}=\dfrac{(k_s+2k_f)-2\phi(k_f-k_s)}{(k_s+2k_f)+\phi(k_f-k_s)}$
Electrical Conductivity	$\dfrac{\sigma_{nf}}{\sigma_f}=1+\dfrac{3\left(\dfrac{\sigma_s}{\sigma_f}-1\right)\phi}{\left(\dfrac{\sigma_s}{\sigma_f}+2\right)-\left(\dfrac{\sigma_s}{\sigma_f}-1\right)\phi}$

Table 2

Nanoparticles and base fluid thermophysical properties [10, 16]

Physical Properties	$\rho\left(\dfrac{\mathrm{kg}}{\mathrm{m}^3}\right)$	$c_p\left(\dfrac{\mathrm{J}}{\mathrm{kg\ K}}\right)$	$k\left(\dfrac{\mathrm{W}}{\mathrm{m\ K}}\right)$	$\sigma\left(\dfrac{\mathrm{S}}{\mathrm{m}}\right)$
H_2O	997.1	4179	0.613	5.5×10^{-6}
Cu	8933	385	401	59.6×10^{6}

3. NUMERICAL PROCEDURE

Here we employed shooting technique together with the Runge-Kutta-Fehlberg integration scheme in order to solve the model equations (7)–(10). The procedure involves transforming the model boundary value problem into a system of initial value problem. Let

$$x_1 = F(\xi),\ \ x_2 = F'(\xi),\ \ x_3 = F''(\xi),\ \ x_4 = \theta(\xi),\ \ x_5 = \theta'(\xi). \tag{12}$$

Equations (7)–(10) then become

$$\begin{gathered} x_1' = x_2,\ \ x_2' = x_3,\ \ x_4' = x_5,\quad x_3' = A_0 A_1 M\left(x_2 - 1\right) + A_0\left(1 - S\right) - A_0\left(x_1 x_3 - x_2^2\right) - A_0 S\left(x_2 + \frac{\xi+1}{2} x_3\right), \\ x_5' = -A_2 x_5 Pr\left(x_1 + \frac{\xi+1}{2}\right) - A_3 x_3^2 (\mathrm{Pr})(\mathrm{Ec}) - A_4 (\mathrm{Pr})(\mathrm{Ec}) M\left(x_2 - 1\right)^2, \end{gathered} \tag{13}$$

with the initial conditions,

$$x_1(0) = 0,\quad x_2(0) = \lambda + L x_3(0),\quad x_3(0) = a_1,\quad x_4(0) = a_2,\quad x_5(0) = \mathrm{Bi}\left(a_2 - 1\right). \tag{14}$$

The unknown values of a_1 and a_2 are first guessed and subsequently obtained via shooting numerical procedure using Newton Raphson root finding method. Thereafter, the system of first order ODEs is then numerically solved by applying Runge-Kutta-Fehlberg integration scheme [22].

4. RESULTS AND DISCUSSION

This section deals with the physical interpretations of the pertinent results obtained from the numerical computations. In order to validate the accuracy of our numerical results, we compare a special case of our results when $M = S = \phi = L = 0$ with those reported by [2, 14, 21] as reflected in table 1, and a favorable agreement is achieved.

Table 3

Computations showing comparison for stretching surface with $M = S = \phi = L = 0$

λ	Ref. [14] $\sqrt{\mathrm{Re}_x} C_f$	Ref. [2] $\sqrt{\mathrm{Re}_x} C_f$	Ref. [21] $\sqrt{\mathrm{Re}_x} C_f$	Present results $\sqrt{\mathrm{Re}_x} C_f$
0	1.232588	1.232588	1.232588	1.23258766
0.1	1.14656	1.146561	1.146561	1.14656100
0.2	1.05133	-	1.051130	1.05112999
0.5	0.71330	0.713295	0.713295	0.71329496
0.8	-	0.306095	0.306095	0.30609476
1	0	0	0	0
2	–1.88731	–1.887307	–1.887307	–1.88730667

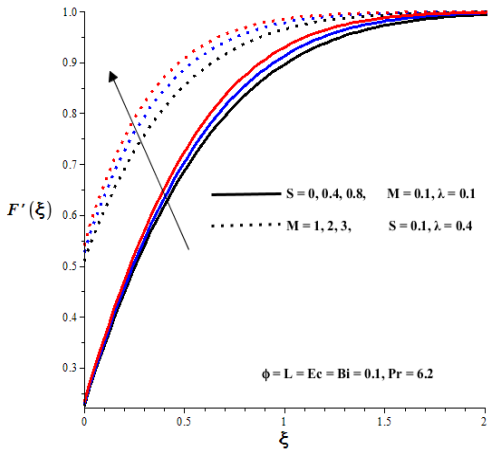

Fig. 2 – The impact of S and M on the velocity profile of Cu-water nanofluid flow.

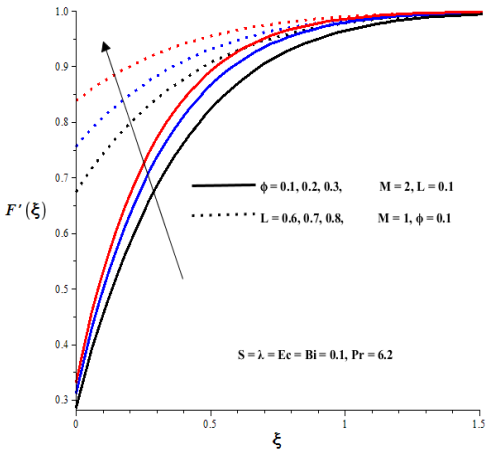

Fig. 3 – The impact of ϕ and L on the velocity profile of Cu-water nanofluid flow.

The effects of emerging parameters on the Cu-water nanofluid velocity profiles are displayed in Figs. 2 and 3. Generally, the velocity profiles increase from the sheet surface and attained its maximum free stream value. Meanwhile, a reduction in the velocity boundary layer thickness is observed in both Figs. 2 and 3 with an increase in value of S (vertical movement of the surface), M (magnetic field), ϕ (nanoparticle volume fraction) and L (surface slipperiness). It is noteworthy that a decrease in velocity boundary layer thickness will enhance the interaction between Cu-water nanofluid and the heated surface leading an elevation in heat transfer rate.

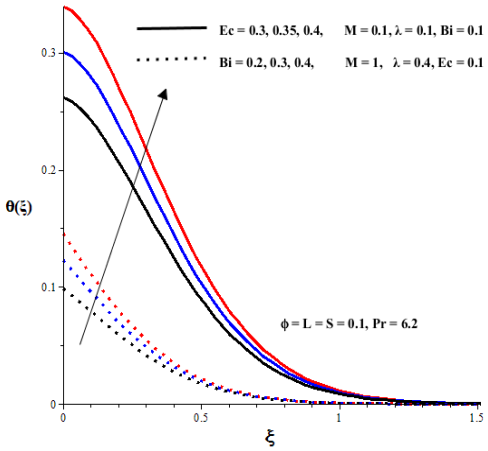

Fig. 4 – The impact of *Ec* and *Bi* on the temperature profile of Cu-water nanofluid flow.

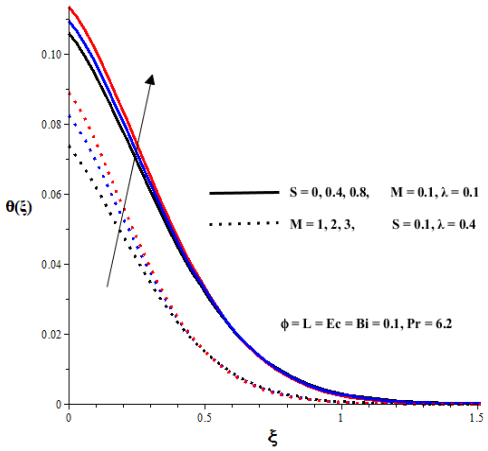

Fig. 5 – The impact of S and M on the temperature profile of Cu-water nanofluid flow.

From the temperature profiles as shown in Figs. 4–6, it is observed in general that the Cu-water nanofluid temperature is maximum at the sheet surface due convective heating and decreases gradually towards the free stream temperature far away from the surface. Figures 4–6 revealed that both the sheet surface temperature and Cu-water thermal boundary layer thickness upsurge with a rise in the values of Ec (Eckert number), Bi (Biot number), S (vertical movement of the surface), M (magnetic field), and ϕ (nanoparticle volume fraction). The elevation in the Cu-water temperature within the boundary layer region can be attributed to the combined effects of convective heating of the sheet surface due to hot fluid underneath, viscous dissipation, Joule heating due to magnetic field and nanoparticles thermal conductivity, hence, the thermal boundary layer thickness is enhanced. Moreover, an increase in value of L (surface slipperiness) lessens the nanofluid temperature, consequently, the thermal boundary layer thickness diminished.

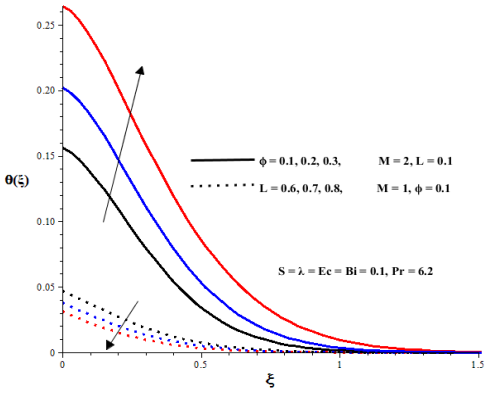

Fig. 6 – The impact of ϕ and L on the temperature profile of Cu-water nanofluid flow.

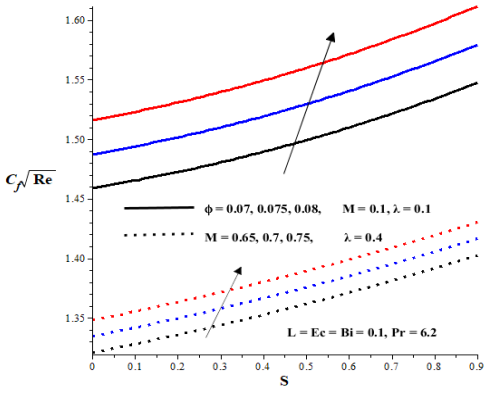

Fig. 7 – The impact of ϕ, M and S on the skin friction between Cu-water nanofluid flow and the heated surface.

The effects of various thermophysical parameters on the sheet surface skin friction are depicted in Fig. 7. Interestingly, the skin friction escalates with a rise in the parameter value of ϕ (nanoparticle volume fraction), M (magnetic field), and S (vertical movement of the surface). This can be attributed to an elevation in the velocity gradient at the sheet surface as the values of these parameters increase.

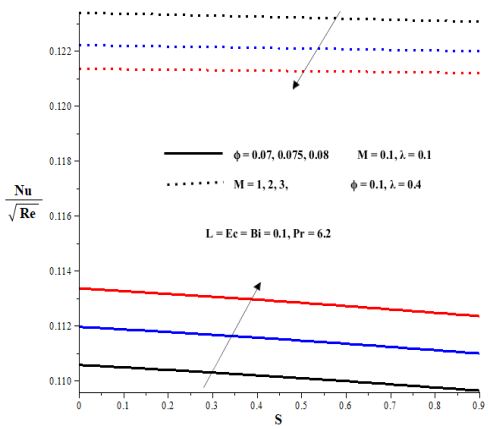

Fig. 8 – The impact of ϕ, *M* and *S* on the Nusselt number of Cu-water nanofluid flow.

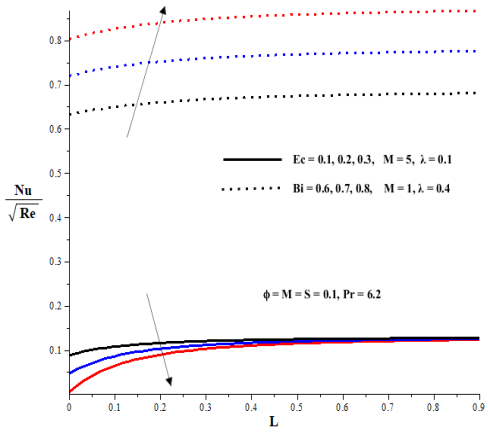

Fig. 9 – The impact of *Ec*, *Bi* and *L* on the Nusselt number of Cu-water nanofluid flow.

Figures 8 and 9 depict the parameters variation effects on the Nusselt number. This represents the heat transfer rate at the convectively heated sheet surface. The heat flux at the sheet surface increases with an elevation in value of ϕ (nanoparticle volume fraction), Bi (Biot number) and *L* (surface slipperiness), while a rise in the value of *M* (magnetic field), *S* (vertical movement of the surface) and Ec (Eckert number) lessens the Nusselt number. This may be attributed to an increase or decrease in the temperature gradient at the sheet surface as these parameters value varies.

Figures 10–12 shows the total irreversibility due to heat transfer together with the fluid friction and magnetic field known as entropy generation rate. In general, the entropy generation is maximum at the sheet surface and decreases gradual to zero value outside the boundary layer region at the free stream. The heighten in entropy generation at the sheet surface may be due to the combined effects of heat transfer and nanofluid friction with magnetic field irreversibility. An increase in values of ϕ (nanoparticle volume fraction), Ec (Eckert number), Bi (Biot number), *S* (vertical movement of the surface) and *M* (magnetic field) boost the entropy generation rate within the boundary layer. On contrary, the entropy generation diminished with a rise in value of *L* (surface slipperiness).

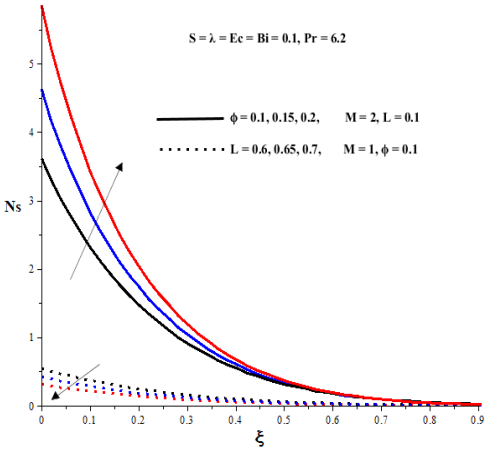

Fig. 10 – The impact of ϕ and *L* on the entropy generation produced by Cu-water nanofluid flow.

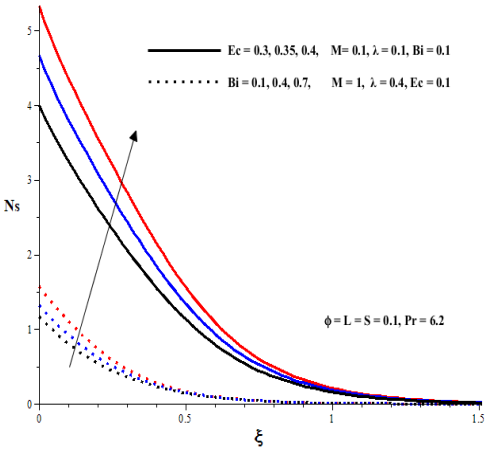

Fig. 11 – The impact of Ec and Bi on the entropy generation produced by Cu-water nanofluid flow.

Generally speaking, the Bejan number value ranges from 0 to 1. The Bejan number less than 0.5 implies the nanofluid fluid friction and magnetic field irreversibility dominate the entropy generation, while the Bejan number greater than 0.5 implies the domination of heat transfer irreversibility. Figures 13–15 revealed that the Bejan number attained its maximum value within the boundary layer region and its lowest zero value at the free stream. It is interesting to note that the values of the Bejan number is less than 0.5 in general. Consequently,

fluid friction with magnetic field irreversibility dominate the entropy generation in the entire flow regime. Meanwhile, an increase in the parameter values of S (vertical movement of the surface), M (magnetic field), L (surface slipperiness), ϕ (nanoparticle volume fraction, Ec (Eckert number) and Bi (Biot number) enhanced the Bejan number within the boundary layer, thus, augment the contribution of heat transfer irreversibility to entropy generation.

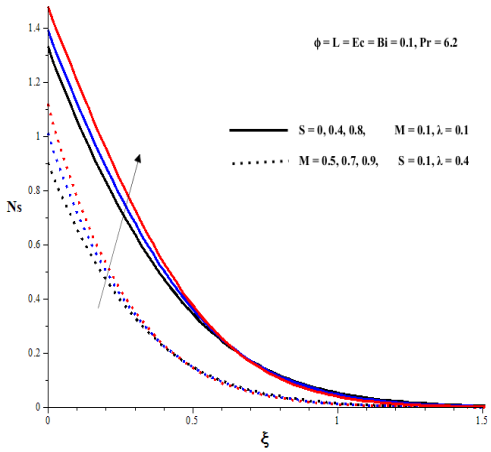

Fig. 12 – The impact of S and M on the entropy generation produced by Cu-water nanofluid flow.

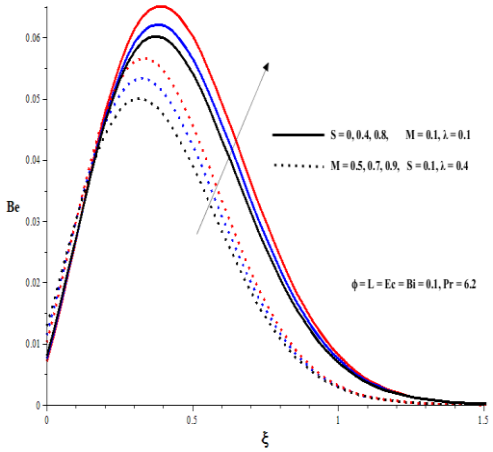

Fig. 13 – The impact of S and M on the Bejan number.

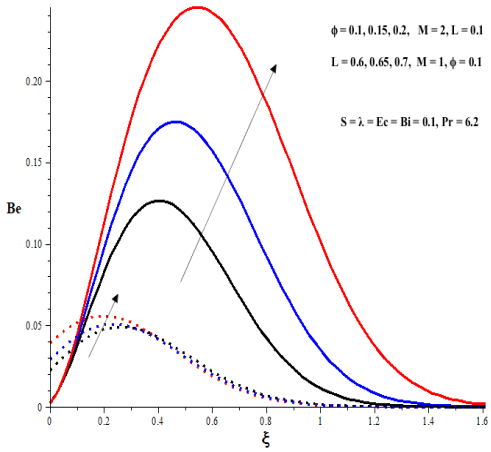

Fig. 14 – The impact of ϕ and L on the Bejan number.

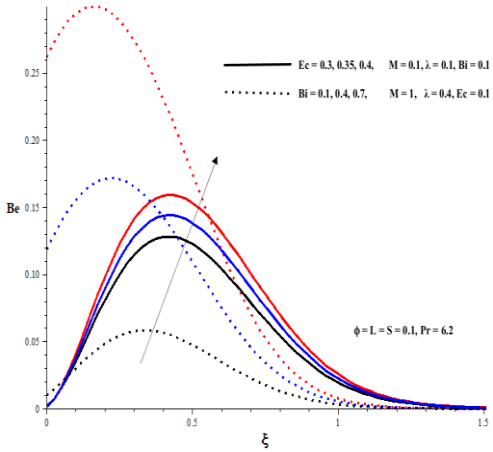

Fig. 15 – The impact of S and M on the Bejan number.

5. CONCLUSION

A theoretical study was conducted on the unsteady MHD Cu-water nanofluid convection and heat transfer with entropy generation over an upward and downward moving stretchable slippery surface. The model problem was numerically tackled via the shooting method with Runge-Kutta-Fehlberg integration scheme. The main findings can be summarized as follows:

- The velocity boundary layer thickness lessened with an increase in the value of S, M, ϕ and L.
- The thermal boundary layer thickness amplified with an upsurge in value of Ec, Bi, S, M, and ϕ. An increase in the value of L lessened the thermal boundary layer thickness.
- The skin friction at the sheet surface escalates with a rise in the value of ϕ, M, and S.
- The Nusselt number is enhanced with a rise in the value of ϕ, Bi, and L. An increase in value of M, S and Ec diminished the Nusselt number.
- The entropy generation within the boundary layer escalates with an increase in the value of ϕ, Ec, Bi, S and M but decreases with increase in the value of L.

- The Bejan number escalates with an increase in value of S, M, L, ϕ, Ec and Bi.

Finally, it is noteworthy that the heat transfer enhancement capability and entropy generation minimization in a conducting nanofluid convection in the presence of magnetic field can be achieved by optimally regulating the values of various embedded parameters. This will innovatively boost the coolant effectiveness in various engineering and industrial applications.

REFERENCES

1. S.U.S. CHOI, *Enhancing thermal conductivity of fluids with nanoparticles, development and application of non-Newtonian flow*, ASME Journal of Heat Transfer, **66**, pp. 99–105, 1995.
2. A. ISHACK, *Dual solution in the stagnation point flow over a shrinking sheet*, International Journal of Mathematical Models and Methods in Applied Science, **12**, pp. 56–59, 2018.
3. J.H. MERKIN, I. POP, Y.Y. LOK, T. GROSAN, *Similarity solutions for the boundary layer flow and heat transfer of viscous fluids, porous media, and micropolar fluids*, Elsevier, Oxford, UK, 2021
4. A. SHEREMET, I. POP, *Convective flow and heat transfer from wavy surfaces: viscous fluids, porous, and nanofluids*, CRC Press, Boca Raton, 2016.
5. J. BUONGIORNO, *Convective transport in nanofluids*, ASME J. Heat Transf., **128**, pp. 240–250, 2006.
6. T. KHAMLICHE, S. KHAMLICHE, T.B. DOYLE, O.D. MAKINDE, M. MAAZA, *Thermal conductivity enhancement of nano-silver particles dispersed ethylene glycol based nanofluids*, Materials Research Express, **5**, *3*, art. 035020, 2018.
7. H.U. KANG, S. H. KIM, J.M. OH, *Estimation of thermal conductivity of nanofluid using experimental effective particle volume*, Exp. Heat Transfer **19**, pp. 181–191, 2006**.**
8. S. RASHIDI, *Magnetohydrodynamics flow and heat transfer around a solid cylinder wrapped with a porous ring*, Journal of heat transfer, **136**, *6*, art. 062601, 2014.
9. M.K. NAYAK, F. MABOOD, W.A. KHAN, O.D. MAKINDE, *Cattaneo-Christov double diffusion on micropolar magneto cross nanofluids with entropy generation*, Indian Journal of Physics, **96**, pp. 193–208, 2022.
10. T. ZUBAIR, M. USMAN, K.S. NISAR, M. HAMID, E.E. MAHMOUD, I.S. YAHIA, *Investigation of shape effects of Cu-nanoparticle on heat transfer of MHD rotating flow over nonlinear stretching sheet*, Alexandria Engineering Journal, **61**, *6*, pp. 4457–4466, 2022.
11. T. SALAHUDDIN, M.H.U. KHAN, M. KHAN, B.A. ALWAN, A. AMARI, *An analysis on the flow behavior of MHD nanofluid with heat generation*, Fuel, **311**, art. 122548, 2022.
12. R.P. SHARMA, S. MISHRA, *Analytical approach on magnetohydrodynamic Casson fluid flow past a stretching sheet via Adomian decomposition method*, Heat Transfer, **51**, *2*, pp. 2155–2164, 2022.
13. R. SARAVANA, R.H. REDDY, K.V.N. MURTHY, O.D. MAKINDE, *Thermal radiation and diffusion effect in MHD Williamson and Casson fluid flows past a slandering stretching surface*, Heat Transfer, **51**, *4*, pp. 3187–3200, 2022.
14. Y.Y. LOK, A. ISHACK, I. POP, *MHD stagnation point flow towards a shrinking sheet*, International Journal of Numerical Methods for Heat and Fluid Flow, **21**, *1*, pp. 61–72, 2011.
15. N.S. ANUAR, N. BACHOK, N.M. ARIFIN, H. ROSALI, *MHD flow past a nonlinear stretching/shrinking sheet in carbon nanotubes: Stability analysis*, Chinese journal of physics, **65**, pp. 436–446, 2020.
16. F.B. TADESSE, O. MAKINDE, L.G. ENYADENE, *Hydromagnetic stagnation point flow of a magnetite ferrofluid past a convectively heated permeable stretching/shrinking sheet in a Darcy-Forchheimer porous medium*, Sādhanā – Academy Proceeding in Engineering Science, **46**, art. 115, 2021.
17. F.B. TADESSE, O.D. MAKINDE, L.G. ENYADENE, *Mixed convection of a radiating magnetic nanofluid past a heated permeable stretching/shrinking sheet in a porous median*, Mathematical problems in Engineering, **2021**, art. 6696748, 2021.
18. S. NANDI, B. KUMBHAKAR, S. SARKAR, *MHD stagnation point flow of Fe_3O_4/Cu/Ag-CH_3OH nanofluid along a convectively heated stretching sheet with partial slip and activation energy: Numerical and statistical approach*, International Communications in Heat and Mass Transfer, **130**, art. 105791, 2022.
19. H. GUL, M. RAMZAN, K.S. NISAR, R.N. MOHAMED, H.A.S. GHAZWANI, *Performance-based comparison of Yamada-Ota and Hamilton-Crosser hybrid nanofluid flow models with magnetic dipole impact past a stretched surface*, Scientific Reports, **12**, art. 29, 2022.
20. N.S. KHASHI'IE, N.M. ARIFIN, I. POP, *Magnetohydrodynamics (MHD) boundary layer flow of hybrid nanofluid over a moving plate with joule heating*, Alexandria Engineering Journal, **61**, *3*, pp. 1938–1945, 2022.
21. K.S. TSHIVHI, O.D. MAKINDE, *Magneto-nanofluid coolants past heated shrinking/stretching surface: Dual solution and stability analysis*, Results in Engineering, **10**, art. 100229, 2021.
22. T.Y. NA, *Computational methods in engineering boundary value problem*, Academic Press, 1979.

Received January 25, 2022